Inorg. Chem. **1986**, *25*, 1617–1623

Contribution from the Department of Chemistry,
University of South Carolina, Columbia, South Carolina 29208

Cluster Synthesis. 11. Role of Sulfido Ligands in the Synthesis of Heteronuclear Clusters. Synthesis and Crystal and Molecular Structures of $PtOs_4(CO)_{11}(PMe_2Ph)_2(\mu_3\text{-}S)_2$ and $PtOs_3(CO)_9(PMe_2Ph)_2(\mu_3\text{-}S)_2$

Richard D. Adams,* István T. Horváth, and Suning Wang

Received October 21, 1985

The synthesis of the mixed-metal cluster compounds $PtOs_4(CO)_{11}(PMe_2Ph)_2(\mu_3\text{-}S)_2$ (**1**) and $PtOs_3(CO)_9(PMe_2Ph)_2(\mu_3\text{-}S)_2$ (**2**) was achieved by the reaction of $Os_4(CO)_{12}(\mu_3\text{-}S)_2$ (**3**) with $Pt(PMe_2Ph)_4$. Compound **1** was converted into **2** by treatment with CO. Compound **2** was also synthesized by the reaction of $Os_3(CO)_9(\mu_3\text{-}S)_2$ with $Pt(PMe_2Ph)_4$. Compounds **1** and **2** were characterized structurally by single-crystal X-ray diffraction analyses. For **1**: space group $Pca2_1$, No. 29; a = 23.801 (3) Å, b = 9.136 (3) Å, c = 18.368 (4) Å, Z = 4, ρ_{calcd} = 2.81 g/cm³. The structure was solved by direct methods (MULTAN) and refined (2343 reflections, $F^2 \geq 3.0\sigma(F^2)$) to the final residuals R_F = 0.040 and R_{wF} = 0.042. For **2**: space group $P2_1/c$, No. 14; a = 9.533 (4) Å, b = 15.580 (7) Å, c = 24.547 (8) Å, β = 99.87 (3)°, Z = 4, ρ_{calcd} = 2.51 g/cm³. The structure was solved by direct methods (MULTAN) and refined (2527 reflections, $F^2 \geq 3.0\sigma(F^2)$) to the final residuals R_F = 0.037 and R_{wF} = 0.049. The cluster of **1** consists of a butterfly tetrahedron of four osmium atoms with a $Pt(PMe_2Ph)_2$ group bridging one of the peripheral edges. The cluster of **2** consists of an open triangular cluster of three osmium atoms with a $Pt(PMe_2Ph)_2$ group bridging one of the two osmium–osmium bonds. Variable-temperature ^1H NMR studies of **2** showed that it undergoes a rapid rearrangement of the cluster framework, ΔG_{167} = 7.5 kcal/mol, that produces a time-averaged plane of symmetry. A process in which the platinum atom interchanges bridging sites between the two osmium–osmium bonds is proposed.

Introduction

The development of systematic routes for the synthesis of transition-metal cluster compounds has been one of the foremost challenges of modern inorganic chemistry.[1–5] Redox coupling[2] and pyrolytic condensations[6] have produced a wealth of new compounds. Metal–metal exchange reactions have been used to synthesize a variety of heteronuclear (mixed) metal cluster compounds, eq 1.[3,7]

$$M_xL_a + M'L'_b \rightarrow M_{x-1}M'L_{a-y}L'_{b-z} + ML_yL'_z \qquad (1)$$

While the product of a metal–metal exchange reaction is usually isoelectronic with the starting cluster, these reactions are complex mechanistically due to the occurrence of metal addition and elimination steps as well as ligand exchange processes.[3] Recent studies have indicated that bridging ligands can greatly facilitate metal–metal exchange reactions.[3,4] We have shown that sulfido ligands can be very effective in promoting the synthesis of higher nuclearity osmium clusters through condensation processes.[4] In this report is described the synthesis of the new platinum–osmium clusters $PtOs_4(CO)_{11}(PMe_2Ph)_2(\mu_3\text{-}S)_2$ (**1**) and $PtOs_3(CO)_9(PMe_2Ph)_2(\mu_3\text{-}S)_2$ (**2**) by the reactions of $Os_4(CO)_{12}(\mu_3\text{-}S)_2$ (**3**) and $Os_3(CO)_9(\mu_3\text{-}S)_2$ (**4**) with $Pt(PMe_2Ph)_4$. Compound **2** was found to exhibit an unusually facile dynamical stereochemistry in which the platinum atom moves rapidly between different osmium–osmium bonds in the cluster.[8]

Experimental Section

General Data. Unless otherwise specified, all the reactions were performed under a nitrogen atmosphere. Reagent grade solvents were used without further purification. $Os_4(CO)_{12}(\mu_3\text{-}S)_2$[9] (**3**), $Pt(PMe_2Ph)_4$,[10] and $Os_3(CO)_9(\mu_3\text{-}S)_2$[11] (**4**) were prepared by published methods. ^1H NMR spectra were taken at 80 MHz on an IBM NR-80 spectrometer and at 250 MHz on a Bruker WM-250 FT-NMR spectrometer. ^{31}P NMR spectra were taken at 81 MHz on a Bruker WP200 spectrometer with H_3PO_4 as a external reference. IR spectra were recorded on a Nicolet 5-DXB FTIR spectrophotometer.

Reaction between $Os_4(CO)_{12}(\mu_3\text{-}S)_2$ and $Pt(PMe_2Ph)_4$. To a solution of **3** (40 mg, 0.035 mmol) in 20 mL of CH_2Cl_2 at 25 °C was added a solution of 45 mg of $Pt(PMe_2Ph)_4$ (0.060 mmol) in 5 mL of CH_2Cl_2. The solution was stirred for 20 h at 25 °C and the solvent was then removed in vacuo. The residue was separated by TLC on silica plates with a 30% CH_2Cl_2/70% hexane solution mixture. In order of elution the following compounds were isolated: **3** (unreacted), red, 5 mg, 13%; $Os_4(CO)_{11}(PMe_2Ph)(\mu_3\text{-}S)_2$,[12] red, 5 mg, 11%; $PtOs_3(CO)_9(PMe_2Ph)_2(\mu_3\text{-}S)_2$ (**2**), yellow, 8 mg, 17%; $PtOs_4(CO)_{11}(PMe_2Ph)_2(\mu_3\text{-}S)_2$ (**1**), red, 5 mg, 9%.

Crystals of **1** containing 1 mol of CH_2Cl_2 solvent/mol of complex were obtained by cooling a solution in a 10% CH_2Cl_2/90% hexane solvent mixture to −20 °C. Anal. Calcd: C, 19.89; H, 1.42. Found: C, 21.24; H, 1.44. Crystals of **2** containing $^1/_2$ mol of hexane solvent/mol of complex were obtained by slow evaporation of a solution containing a 20%/80% benzene/hexane solvent mixture at 0 °C. Anal. Calcd: C, 23.98; H, 2.07. Found: C, 23.85; H, 1.96.

Reaction of $Os_3(CO)_9(\mu_3\text{-}S)_2$ (4) with $Pt(PMe_2Ph)_4$. A solution containing **4** (40 mg, 0.045 mmol), $Pt(PMe_2Ph)_4$ (50 mg, 0.067 mmol), and 30 mL of CH_2Cl_2 was stirred at 25 °C under a CO atmosphere for 16 h. The solvent was removed in vacuo, and the residue was separated by TLC on silica plates with a 20%/80% CH_2Cl_2/hexane solvent mixture. This yielded the following compounds: unreacted starting material $Os_3(CO)_9(\mu_3\text{-}S)_2$ (**4**) 8 mg, 20%; $Os_3(CO)_8(PMe_2Ph)(\mu_3\text{-}S)_2$, 2 mg, 4%; $Os_3(CO)_7(PMe_2Ph)_2(\mu_3\text{-}S)_2$, 16 mg, 32%; and **2**, 11 mg, 18%.

Reaction between 2 and $Os(CO)_5$. To 30 mL of a hexane solution containing 20 mg (0.014 mmol) of **2** was added 6 mL of a heptane solution of $Os(CO)_5$ (~0.03 mmol/mL, 0.18 mmol). This solution was purged with N_2 and irradiated (UV) for 1 h at 10 °C. After the removal of the solvent in vacuo, the residue was separated by TLC on silica plates with 30%/70% CH_2Cl_2/hexane. Three major bands were separated: red-orange $Os_4(CO)_{13}(\mu_3\text{-}S)_2$, 2 mg, 12%; yellow **2**, 10 mg, 50%; red **1**, 4 mg, 18%.

Reaction of 1 with CO. A 10-mg sample of **1** was dissolved in 5 mL of CH_2Cl_2 at 25 °C and stirred for 20 h under a CO atmosphere. The reaction mixture was separated by TLC on silica plates with a 30%/70% CH_2Cl_2/hexane solvent mixture. The principal products were $Os_4(CO)_{13}(\mu_3\text{-}S)_2$ (2 mg, 27%) and **2** (2 mg, 24%).

Variable-Temperature ^1H NMR for Compound 2. Variable-temperature ^1H NMR spectra of compound **2** were run on a Bruker WH-400 spectrometer on samples dissolved in a 1/1 CH_2Cl_2/CF_2Cl_2 solvent mixture. The temperatures were calibrated externally by using a copper–constantan thermocouple. The activation energy was calculated by using the coalescence temperature, 167 K, and the chemical shift separation of the two low-field resonances at 155 K.

Crystallographic Analysis. Data crystals were mounted in thin-walled glass capillaries. Diffraction measurements were made on a Enraf-

---

(1) *Transition Metal Clusters*; Johnson, B. F. G., Ed.; Wiley: Chichester, England, 1980; Chapter 1.
(2) Chini, P.; Longoni, G.; Albano, V. G. *Adv. Organomet. Chem.* **1976**, *14*, 285.
(3) Vahrenkamp, H. *Adv. Organomet. Chem.* **1983**, *22*, 169.
(4) Adams, R. *Polyhedron* **1985**, *4*, 2003.
(5) King, R. B. *Prog. Inorg. Chem.* **1972**, *15*, 287.
(6) Eady, C. R.; Johnson, B. F. G.; Lewis, J. *J. Chem. Soc., Dalton Trans.* **1975**, 2606.
(7) Horwitz, C. P.; Holt, E. M.; Shriver, D. F. *Organometallics* **1985**, *4*, 1117.
(8) Adams, R. D.; Wang, S. *Inorg. Chem.* **1985**, *24*, 4447.
(9) Adams, R. D.; Horváth, I. T.; Mathur, P.; Segmuller, B. E.; Yang, L.-W. *Organometallics* **1983**, *2*, 1078.
(10) Clark, H. C.; Itoh, K. *Inorg. Chem.* **1971**, *10*, 1707.
(11) Adams, R. D.; Horváth, I. T.; Mathur, P.; Segmuller, B. E.; Yang, L.-W. *Organometallics* **1983**, *2*, 1301.
(12) Adams, R. D.; Horváth, I. T.; Natarajan, K. *Organometallics* **1984**, *3*, 1540.
(13) Adams, R. D.; Horváth, I. T.; Segmuller, B. E.; Yang, L.-W. *Organometallics* **1983**, *2*, 144.

0020-1669/86/1325-1617$01.50/0

Table I. Crystallographic Data for X-ray Diffraction Studies

	1	2
	(A) Crystal Data	
formula	$PtOs_4S_2P_2O_{11}C_{28}H_{22}\cdot CH_2Cl_2$	$PtOs_3S_2P_2O_9C_{25}H_{22}$
temp (±3), °C	23	23
space group	$Pca2_1$, No. 29	$P2_1/c$, No. 14
a, Å	23.801 (3)	9.533 (4)
b, Å	9.136 (3)	15.580 (7)
C, Å	18.368 (4)	24.547 (8)
α, deg	90.0	90.0
β, deg	90.0	99.87 (3)
γ, deg	90.0	90.0
V, Å^3	3994 (3)	3592 (5)
M_r	1689.37	1358.21
Z	4	4
ρ_{calcd}, g/cm^3	2.81	2.51
	(B) Measurement of Intensity Data	
radiation	Mo Kα (0.71073 Å)	Mo Kα (0.71073 Å)
monochromator	graphite	graphite
detector aperture, mm		
horiz ($A + B$ tan θ)		
A	3.0	3.0
B	1.0	1.2
vert	4.0	4.0
cryst faces	$001,00\bar{1},201,\bar{2}0\bar{1}$ $1\bar{1}0,\bar{1}20,\bar{1}1\bar{1}$	$001,00\bar{1},010$ $0\bar{1}0,110,\bar{2}\bar{1}0$
cryst size, mm	0.17 × 0.20 × 0.30	0.05 × 0.17 × 0.25
crystal orientation direction; deg from ϕ axis	b; 9.9	[$20\bar{1}$]; 6.15
reflcns measd	$+h,+k,+l$	$+h,+k,\pm l$
max 2θ, deg	50	47
scan type	moving cryst–stationary counter	moving cryst–stationary counter
ω-scan width (A + 0.347 tan θ), deg	1.10	1.00
bkgd	$^1/_4$ addnl scan at each end of scan	$^1/_4$ addnl scan at each end of scan
ω-scan rate (variable), deg/min		
max	10.0	10.0
min	1.7	1.5
no. of reflcns measd	3973	5896
no. of data used ($F^2 \geq 3.0\sigma(F)$)	2343	2527
	(C) Treatment of Data	
abs cor		
coeff, cm^{-1}	165.9	147.8
grid	14 × 10 × 6	14 × 12 × 4
transmissn coeff		
max	0.124	0.475
min	0.025	0.056
P factor	0.02	0.03
final residuals		
R_F	0.040	0.037
R_{wF}	0.042	0.049
esd of unit wt observn	1.520	1.631
largest shift/error value of final cycle	0.00	0.01
largest peak in final diff Fourier, e/Å^3	0.98	1.73

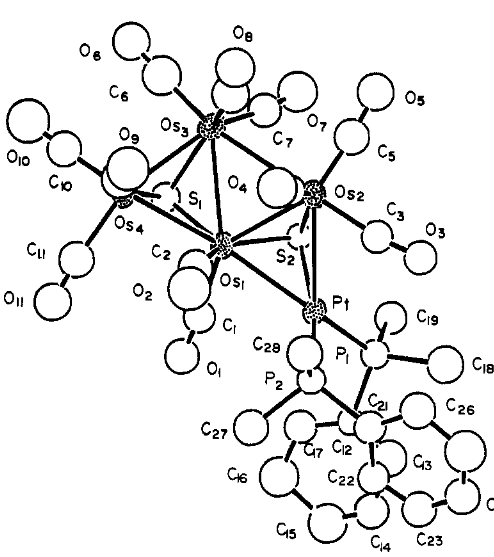

Figure 1. ORTEP diagram of $PtOs_4(CO)_{11}(PMe_2Ph)_2(\mu_3\text{-}S)_2$ (**1**) showing 50% probability thermal motion ellipsoids.

Nonius CAD-4 fully automated four-circle diffractometer using graphite monochromatized Mo Kα radiation. Unit cells were determined and refined from 25 randomly selected reflections obtained by using the CAD-4 automatic search, center, index, and least-squares routines. Crystal data, data collection parameters, and results of the analyses are listed in Table I. All data processing was performed on a Digital Equipment Corp. VAX 11/782 computer by using the Enraf-Nonius SDP program library. Absorption corrections of a Gaussian integration type were done for both structures. Neutral-atom scattering factors were calculated by the standard procedures.[14a] Anomalous dispersion corrections were applied to all non-hydrogen atoms.[14b] Full-matrix least-squares refinements minimized the function

$$\sum_{hkl} w(|F_o| - |F_c|)^2$$

where $w = 1/\sigma(F)^2$, $\sigma(F) = \sigma(F_o^2)/2F_o$, and $\sigma(F_o^2) = [\sigma(I_{raw})^2 + (PF_o^2)^2]^{1/2}/Lp$.

For compound **1** the systematic absences in the data were consistent either with the space group $Pca2_1$, or with $Pbcm$. Because of the expected low symmetry of the molecule the former alternative was chosen. This choice was assumed to be correct on the basis of the successful structure solution and refinement. The heavy atoms of the molecule were located in an E map based on the phasing of 236 reflections ($E \geq 1.77$) by a direct methods calculation (MULTAN). All remaining non-hydrogen atoms were obtained by difference Fourier syntheses. Due to the limited size of the data set for compound **1** only the metal atoms were refined with anisotropic thermal parameters and the hydrogen atom contributions were ignored.

For compound **2** the systematic absences that were observed in the data were consistent only with the space group $P2_1/c$. The metal atoms in the structure of **2** were located in an E map based on the phasing of 369 reflections ($E \geq 1.87$) by direct methods (MULTAN). The positions of the remaining non-hydrogen atoms were located by difference Fourier syntheses. For **2** all atoms heavier than oxygen refined anisotropically. Hydrogen atom contributions were included in the structure factor calculations, but their positions were not refined. A structure factor table for the structure analysis of compound **1** is available; see the paragraph at the end of this paper regarding supplementary material. The structure factor table for compound **2** was published previously.[8]

Results

The reaction of $Os_4(CO)_{12}(\mu_3\text{-}S)_2$,[3] with $Pt(PMe_2Ph)_4$ in methylene chloride solvent at 25 °C yields the mixed-metal cluster compounds $PtOs_4(CO)_{11}(PMe_2Ph)_2$ $(\mu_3\text{-}S)_2$ (**1**) in 9% yield, $PtOs_3(CO)_9(PMePh)_2(\mu_3\text{-}S)_2$ (**2**) in 17% yield, and the phosphine substitution product of **2**, $Os_4(CO)_{11}(PMe_2Ph)(\mu_3\text{-}S)_2$.[12] Compounds **1** and **2** have been characterized by IR, ^1H NMR, and ^{31}P NMR spectroscopies, elemental analyses, and single-crystal X-ray diffraction analyses. The spectroscopic results are listed in Table II.

Description of the Structure of 1. Final fractional atomic coordinates are listed in Table III. Interatomic distances and angles are listed in Tables IV and V, respectively. An ORTEP drawing of the molecular structure of **1** is shown in Figure 1. The

---

[14] *International Tables for X-ray Crystallography*; Kynoch: Birmingham, England, 1975; Vol. IV: (a) Table 2.2B, pp 99–101; (b) Table 2.3.1, pp 149–150.

Table II. IR and ^{1}H and ^{31}P NMR Spectroscopic Data

compd	^{1}H NMR, δ	^{31}P NMR,^{a} δ	IR (ν_{CO}),^{b} cm^{-1}
$PtOs_4(CO)_{11}(PMe_2Ph)_2(\mu_3\text{-}S)_2$ (**1**)	7.36–7.17 (m, C_6H_5),^{c} 2.35 (d, t, CH_3; J_{P-H} = 10 Hz; J_{Pt-H} = 36 Hz), 1.99 (d, t, CH_3; J_{P-H} = 10 Hz, J_{Pt-H} = 32 Hz), 1.84 (d, t, CH_3; J_{P-H} = 10 Hz, J_{Pt-H} = 32 Hz), 1.49 (d, t, CH_3; J_{P-H} = 11 Hz, J_{Pt-H} = 36 Hz)	−8.45^c (J_{P-P} = 22 Hz, J_{Pt-P} = 3952 Hz); −14.39 (J_{P-P} = 22 Hz, J_{Pt-P} = 3400 Hz)	2074 (s), 2052 (vs), 2031 (s), 1999 (s), 1982 (s), 1954 (m)
$PtOs_3(CO)_9(PMe_2Ph)_2(\mu_3\text{-}S)_2$ (**2**)	7.34–6.93 (m, C_6H_5),^{d} 2.26 (d, t, CH_3; J_{P-H} = 9.8 Hz, J_{Pt-H} = 29.9 Hz), 1.72 (d, t, CH_3; J_{P-H} = 9.9 Hz, J_{Pt-H} = 32.7 Hz)	2.93^c (J_{P-P} = 27 Hz, J_{Pt-P} = 3547 Hz), −14.70 (J_{P-P} = 27 Hz, J_{Pt-P} = 3166 Hz)	2075 (m), 2056 (vs), 2024 (s), 1999 (m), 1982 (w), 1971 (s), 1962 (m), 1948 (w), 1923 (w)

^{a}Vs. H_3PO_4 external. ^{b}In hexane. ^{c}In $CDCl_3$. ^{d}In CD_2Cl_2.

Table III. Positional Parameters and Their Esd's for $PtOs_4(CO)_{11}(PMe_2Ph)_2(\mu_3\text{-}S)_2$ (**1**)

atom	*x*	*y*	*z*	*B*,^{a} Å^2
Pt(1)	0.58695 (4)	0.1445 (1)	0.41027 (8)	2.77 (2)
Os(1)	0.66919 (4)	0.3388 (1)	0.366	2.81 (2)
Os(2)	0.68494 (4)	0.0668 (1)	0.31817 (8)	3.12 (2)
Os(3)	0.74317 (4)	0.3301 (1)	0.24231 (9)	3.60 (2)
Os(4)	0.76404 (4)	0.5205 (1)	0.35581 (9)	3.91 (3)
S(1)	0.6844 (3)	0.5256 (9)	0.2869 (5)	3.9 (2)*
S(2)	0.6035 (3)	0.2121 (8)	0.2975 (4)	2.9 (1)*
Cl(1)	0.9545 (8)	0.463 (2)	0.280 (1)	16.5 (6)*
Cl(2)	1.0441 (7)	0.303 (2)	0.227 (1)	14.7 (6)*
P(1)	0.4970 (3)	0.0670 (9)	0.4044 (5)	3.9 (2)*
P(2)	0.6003 (3)	0.092 (1)	0.5364 (5)	3.5 (2)*
C(1)	0.619 (1)	0.445 (4)	0.429 (2)	4.7 (7)*
O(1)	0.5883 (8)	0.523 (3)	0.462 (1)	5.6 (5)*
C(2)	0.715 (1)	0.330 (4)	0.446 (2)	5.3 (8)*
O(2)	0.740 (1)	0.291 (3)	0.506 (2)	8.0 (7)*
C(3)	0.649 (1)	−0.096 (3)	0.364 (2)	4.5 (7)*
O(3)	0.6278 (8)	−0.205 (2)	0.386 (1)	4.8 (5)*
C(4)	0.749 (1)	0.037 (3)	0.377 (2)	3.8 (6)*
O(4)	0.7901 (9)	0.012 (3)	0.415 (1)	6.7 (6)*
C(5)	0.703 (1)	−0.042 (4)	0.249 (2)	5.7 (8)*
O(5)	0.7203 (9)	−0.113 (3)	0.197 (2)	6.3 (6)*
C(6)	0.786 (1)	0.450 (4)	0.188 (3)	7 (1)*
O(6)	0.811 (1)	0.530 (3)	0.147 (1)	6.5 (6)*
C(7)	0.700 (1)	0.251 (4)	0.175 (2)	5.2 (8)*
O(7)	0.675 (1)	0.199 (3)	0.122 (2)	7.6 (7)*
C(8)	0.803 (1)	0.193 (4)	0.260 (2)	6.2 (9)*
O(8)	0.8449 (9)	0.125 (3)	0.266 (1)	6.5 (6)*
C(9)	0.825 (1)	0.431 (4)	0.404 (2)	6.0 (9)*
O(9)	0.860 (1)	0.350 (3)	0.428 (2)	7.6 (7)*
C(10)	0.811 (1)	0.656 (3)	0.322 (2)	5.4 (8)*
O(10)	0.835 (1)	0.748 (3)	0.292 (2)	8.5 (8)*
C(11)	0.748 (1)	0.646 (4)	0.443 (2)	5.6 (8)*
O(11)	0.7359 (8)	0.710 (3)	0.496 (2)	6.1 (6)*
C(12)	0.450 (1)	0.172 (3)	0.467 (2)	3.4 (6)*
C(13)	0.405 (1)	0.096 (4)	0.493 (2)	6.3 (9)*
C(14)	0.364 (1)	0.177 (4)	0.540 (2)	5.5 (8)*
C(15)	0.373 (1)	0.307 (5)	0.556 (3)	7 (1)*
C(16)	0.424 (1)	0.400 (5)	0.524 (3)	8 (1)*
C(17)	0.460 (1)	0.309 (4)	0.477 (2)	5.1 (8)*
C(18)	0.484 (1)	−0.135 (4)	0.422 (2)	6.3 (9)*
C(19)	0.466 (1)	0.093 (4)	0.309 (2)	5.1 (8)*
C(21)	0.554 (1)	−0.040 (4)	0.578 (2)	4.3 (7)*
C(22)	0.499 (1)	−0.000 (5)	0.608 (2)	4.5 (6)*
C(23)	0.465 (1)	−0.106 (4)	0.635 (2)	5.3 (8)*
C(24)	0.477 (1)	−0.242 (4)	0.631 (2)	5.4 (8)*
C(25)	0.524 (1)	−0.292 (5)	0.604 (3)	7 (1)*
C(26)	0.568 (1)	−0.193 (4)	0.573 (2)	5.6 (8)*
C(27)	0.593 (1)	0.254 (4)	0.596 (2)	5.4 (8)*
C(28)	0.669 (1)	0.020 (4)	0.562 (2)	5.4 (8)*
C(31)	1.025 (2)	0.430 (6)	0.276 (3)	11 (2)*

^{a}Values marked with an asterisk denote isotropically refined atoms.

Table IV. Interatomic Distances (Å) with Esd's for $PtOs_4(CO)_{11}(PMe_2Ph)_2(\mu_3\text{-}S)_2$ (**1**)

Pt–Os(1)	2.762 (1)	P(1)–C(12)	1.88 (3)
Pt–Os(2)	2.967 (1)	P(1)–C(18)	1.90 (3)
Os(1)–Os(2)	2.665 (1)	P(1)–C(19)	1.91 (3)
Os(1)–Os(3)	2.882 (1)	P(2)–C(21)	1.81 (3)
Os(1)–Os(4)	2.809 (1)	P(2)–C(27)	1.85 (4)
Os(2)–Os(3)	3.106 (2)	P(2)–C(28)	1.83 (3)
Os(3)–Os(4)	2.760 (2)	C(1)–O(1)	1.17 (3)
Pt–P(1)	2.258 (7)	C(2)–O(2)	1.31 (4)
Pt–P(2)	2.386 (8)	C(3)–O(3)	1.19 (4)
Os(1)–S(1)	2.28 (2)	C(4)–O(4)	1.22 (4)
Os(3)–S(1)	2.41 (2)	C(5)–O(5)	1.23 (4)
Os(4)–S(1)	2.28 (2)	C(6)–O(6)	1.20 (4)
Pt–S(2)	2.20 (2)	C(7)–O(7)	1.23 (4)
Os(1)–S(2)	2.32 (2)	C(8)–O(8)	1.18 (3)
Os(2)–S(2)	2.38 (2)	C(9)–O(9)	1.21 (3)
Pt–C(1)	2.87 (3)	C(10)–O(10)	1.16 (4)
Os(1)–C(1)	1.93 (3)	C(11)–O(11)	1.17 (4)
Os(1)–C(2)	1.82 (3)	C(12)–C(13)	1.37 (4)
Os(4)–C(2)	2.68 (3)	C(12)–C(17)	1.29 (3)
Pt–C(3)	2.78 (3)	C(13)–C(14)	1.49 (4)
Os(2)–C(3)	1.91 (3)	C(14)–C(15)	1.24 (4)
Os(2)–C(4)	1.90 (3)	C(15)–C(16)	1.61 (5)
Os(2)–C(5)	1.67 (3)	C(16)–C(17)	1.46 (4)
Os(3)–C(6)	1.80 (4)	C(21)–C(22)	1.46 (4)
Os(3)–C(7)	1.76 (3)	C(21)–C(26)	1.44 (4)
Os(3)–C(8)	1.92 (3)	C(22)–C(23)	1.34 (4)
Os(4)–C(9)	1.88 (3)	C(23)–C(24)	1.28 (4)
Os(4)–C(10)	1.78 (2)	C(24)–C(25)	1.31 (4)
Os(4)–C(11)	2.01 (4)	C(25)–C(26)	1.49 (4)

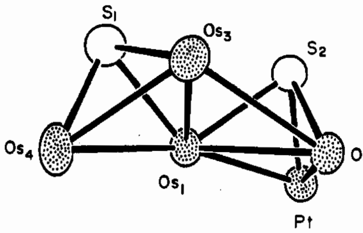

Figure 2. ORTEP diagram of $PtOs_3(CO)_{11}(PMe_2Ph)_2(\mu_3\text{-}S)_2$ (**1**) showing the metal and sulfur atoms.

metal atoms are arranged in an extended array that tends toward planarity but does contain two significant folds; see Figure 2. The amount of folding is revealed from the dihedral angles between the planes Os(1)–Os(2)–Os(3) and Os(1)–Os(3)–Os(4) at 38.7° and Os(1)–Os(2)–Os(3) and Os(1)–Os(2)–Pt at 20.2°. Alternatively, the cluster could be described as a butterfly tetrahedron of four osmium atoms with a $Pt(PMe_2Ph)_2$ group bridging one of the peripheral Os–Os edges. There are seven internuclear separations that are short enough to suggest significant bonding interactions; however, these distances span a wide range. Three of the five osmium–osmium distances, Os(1)–Os(3) = 2.882 (1) Å, Os(1)–Os(4) = 2.809 (1) Å, and Os(3)–Os(4) = 2.760 (2) Å, are typical of those observed in the sulfido-bridged osmium clusters such as **4**, 2.813 (1) Å,[13] and $Os_3(CO)_{10}(\mu_3\text{-}S)$, 2.83 (1) Å.[15] The Os(1)–Os(2) distance at 2.665 (1) Å is short for an electron-precise cluster. This may be influenced by the presence of the several single-atom bridges (Pt, Os(3), and S) that span this interaction. Similarly short bonds have been observed in other

---

(15) Adams, R. D.; Horvâth, I. T.; Kim, H. S. *Organometallics* **1984**, *3*, 548.

Table V. Selected Interatomic Angles (deg) with Esd's for $PtOs_4(CO)_{11}(PMe_2Ph)_2(\mu_3\text{-}S)_2$ (**1**)

Os(1)–Pt–Os(2)	55.29 (3)	Os(3)–Os(1)–S(1)	54.2 (5)	Os(1)–C(1)–O(1)	172 (3)
Pt–Os(1)–Os(2)	66.26 (4)	Os(3)–Os(1)–S(2)	88.0 (5)	Os(1)–C(2)–O(2)	165 (3)
Pt–Os(1)–Os(3)	130.20 (5)	Os(4)–Os(1)–S(1)	52.0 (5)	Os(2)–C(3)–O(3)	172 (3)
Pt–Os(1)–Os(4)	165.85 (5)	Os(4)–Os(1)–S(2)	142.9 (5)	Os(2)–C(4)–O(4)	178 (3)
Os(2)–Os(1)–Os(3)	67.97 (4)	Os(1)–Os(2)–S(2)	54.5 (4)	Os(2)–C(5)–O(5)	174 (3)
Os(2)–Os(1)–Os(4)	114.51 (4)	Os(3)–Os(2)–S(2)	82.0 (4)	Os(3)–C(6)–O(6)	173 (3)
Os(3)–Os(1)–Os(4)	58.01 (4)	Os(1)–Os(3)–S(1)	50.0 (5)	Os(3)–C(7)–O(7)	171 (3)
Pt–Os(2)–Os(1)	58.45 (3)	Os(2)–Os(3)–S(1)	99.4 (4)	Os(3)–C(8)–O(8)	169 (3)
Pt–Os(2)–Os(3)	114.92 (4)	Os(4)–Os(3)–S(1)	51.8 (5)	Os(4)–C(9)–O(9)	168 (2)
Os(1)–Os(2)–Os(3)	59.35 (4)	Os(1)–Os(4)–S(1)	51.9 (5)	Os(4)–C(10)–O(10)	170 (2)
Os(1)–Os(3)–Os(2)	52.69 (3)	Os(3)–Os(4)–S(1)	56.2 (5)	Os(4)–C(11)–O(11)	174 (3)
Os(1)–Os(3)–Os(4)	59.66 (4)	S(2)–Pt–P(1)	102.3 (5)	P(1)–C(12)–C(13)	115 (2)
Os(2)–Os(3)–Os(4)	103.27 (5)	S(2)–Pt–P(2)	161.4 (4)	P(1)–C(12)–C(17)	118 (2)
Os(1)–Os(4)–Os(3)	62.33 (4)	P(1)–Pt–P(2)	93.3 (3)	C(13)–C(12)–C(17)	127 (3)
Os(1)–Pt–S(2)	54.4 (4)	Os(1)–S(1)–Os(3)	75.8 (5)	C(12)–C(13)–C(14)	117 (3)
Os(1)–Pt–P(1)	149.3 (2)	Os(1)–S(1)–Os(4)	76.1 (6)	C(13)–C(14)–C(15)	121 (3)
Os(1)–Pt–P(2)	108.5 (2)	Os(3)–S(1)–Os(4)	72.0 (5)	C(14)–C(15)–C(16)	123 (4)
Os(2)–Pt–S(2)	52.3 (4)	Pt(1)–S(2)–Os(1)	75.3 (6)	C(15)–C(16)–C(17)	111 (3)
Os(2)–Pt–P(1)	130.0 (2)	Pt(1)–S(2)–Os(2)	80.7 (6)	C(12)–C(17)–C(16)	121 (3)
Os(2)–Pt–P(2)	113.7 (2)	Os(1)–S(2)–Os(2)	69.0 (4)	P(2)–C(21)–C(22)	123 (2)
Pt–Os(1)–S(1)	141.4 (5)	C(12)–P(1)–C(18)	107 (1)	P(2)–C(21)–C(26)	118 (2)
Pt–Os(1)–S(2)	50.3 (5)	C(12)–P(1)–C(19)	105 (1)	C(22)–C(21)–C(26)	118 (3)
Pt–Os(2)–S(2)	47.0 (5)	C(18)–P(1)–C(19)	103 (1)	C(21)–C(22)–C(23)	119 (3)
Os(2)–Os(1)–S(1)	117.6 (5)	C(21)–P(2)–C(27)	103 (1)	C(22)–C(23)–C(24)	123 (3)
Os(2)–Os(1)–S(2)	56.5 (4)	C(21)–P(2)–C(28)	102 (1)	C(23)–C(24)–C(25)	123 (4)
S(1)–Os(1)–S(2)	97.5 (7)	C(27)–P(2)–C(28)	103 (1)	C(24)–C(25)–C(26)	122 (4)
				C(21)–C(26)–C(25)	113 (3)

osmium clusters that contain multiple single-atom bridges (e.g. $Os_6(CO)_{16}(\mu_4\text{-}S)(\mu_3\text{-}S)$, 2.686 (1) Å,[16] and $Os_6(CO)_{16}(\mu_4\text{-}CMe)(\mu_3\text{-}CMe)$, 2.672 (6) Å).[17] The Os(2)–Os(3) distance is unusually long, 3.106 (2) Å. This is the only bonding separation that is not bridged by a sulfido ligand. Osmium–osmium bonding distances greater than 3.00 Å have been observed in the electron-rich sulfido clusters $Os_4(CO)_{11}L(\mu_3\text{-}S)_2$, L = CO, PMe_2Ph, and CN-*t*-Bu.[12] Triply bridging sulfido ligands span the triangular groups of metal atoms Os(1)–Os(3)–Os(4) and Os(1)–Os(2)–Pt. Each osmium atom contains three carbonyl ligands except Os(1), which lies in the interior of the cluster and has only two carbonyl ligands. There are only minor deviations from linearity among the carbonyl ligands, but the slight bending of C(2)–O(2) and C(8)–O(8) could be due to weak semibridging interactions. The platinum atom contains two PMe_2Ph ligands. The minor distortions observed in the phenyl ring C(11)–C(16) are believed not to be significant, but the Pt–P(2) bond, which is trans to the sulfido ligand S(2), does seem to be significantly longer than the Pt–P(1) bond, 2.386 (8) vs 2.258 (7) Å.

Under an atmosphere of carbon monoxide, compound **1** undergoes degradation through the loss of one metal atom. Curiously, this seems to be able to occur by both pathways. A loss of osmium leads to **2** while a loss of platinum leads to $Os_4(CO)_{13}(\mu_3\text{-}S)_2$. $Os_4(CO)_{13}(\mu_3\text{-}S)_2$ is known to be formed from **3** by the addition of CO under similar conditions.[18]

Compound **2** was prepared independently in 18% yield through the reaction of $Os_3(CO)_9(\mu_3\text{-}S_2)$ with $Pt(PMe_2Ph)_4$. Details of the molecular structure of **2** were established by an X-ray crystallographic analysis.

Description of the Structure of 2. An ORTEP drawing of **2** is shown in Figure 3. Final fractional atomic coordinates are listed in Table VI. Interatomic distances and angles are listed in Tables VII and VIII, respectively. The structure is very similar to that of the related molecules $PtOs_3(CO)_{11-n}(PPh_3)_n(\mu_3\text{-}S)_2$ (n = 1, 2).[19] The cluster consists of an open triangular cluster of three osmium atoms with a $Pt(PMe_2Ph_2)$ moiety bridging one of the two osmium–osmium bonds. The Pt⋯Os(3) distance at 3.771 (1) Å is clearly nonbonding. The four bonding distances, Pt–Os(1) = 2.936 (1) Å, Pt–Os(2) = 2.789 (1) Å, Os(1)–Os(2) = 3.027 (1) Å, and Os(1)–Os(3) = 2.798 (1) Å, are similar to those found in the PPh_3 derivatives. There were two triply bridging sulfido ligands. S(1) bridges the three osmium atoms, while S(2) is linked to the group Os(2)–Os(3)–Pt. Each osmium atom contains three terminal carbonyl ligands, but C(2)–O(2) and C(6)–O(6) could be engaged in weak semibridging interactions to the platinum atom. The principal difference between **2** and its PPh_3 homologues is that in **2** both phosphine ligands are coordinated to the platinum atom. Unlike those found in **1** the Pt–P distances in **2** are not significantly different.

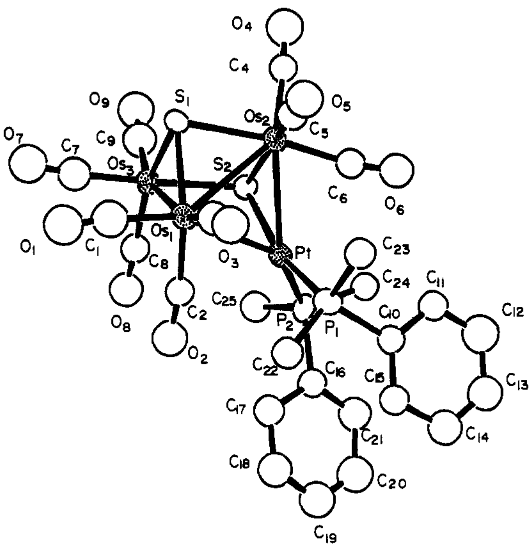

Figure 3. ORTEP diagram of $PtOs_3(CO)_9(PMe_2Ph)_2(\mu_3\text{-}S)_2$ (**2**) showing 50% probability thermal motion ellipsoids.

Since compound **2** is asymmetric, the two phosphine ligands are inequivalent. This was further confirmed by the observation of two resonances at δ = 2.93 and −14.70 in the ^{31}P NMR spectrum at 25 °C. An additional consequence of the absence of symmetry is that all four methyl groups are inequivalent. However, the room-temperature ^1H NMR spectrum showed only two resonances, δ = 2.26 and 1.72, that were appropriately coupled to the ^{31}P and ^{195}Pt nuclei. This anomaly was explained by a

---

(16) Adams, R. D.; Horváth, I. T.; Yang, L.-W. *J. Am. Chem. Soc.* **1983**, *105*, 1533.

(17) Fernandez, J. M.; Johnson, B. F. G.; Lewis, J.; Raithby, P. R. *Acta Crystallogr., Sect. B: Struct. Crystallogr. Cryst. Chem.* **1978**, *B34*, 3086.

(18) Adams, R. D.; Yang, L.-W. *J. Am. Chem. Soc.* **1983**, *105*, 235.

(19) Adams, R. D.; Hor, T. S. A.; Horváth, I. T. *Inorg. Chem.* **1984**, *23*, 4733.

Table VI. Positional and Thermal Parameters for $PtOs_3(CO)_9(PMe_2Ph)_2(\mu_3\text{-}S)_2$ (**2**)

atom	*x*	*y*	*z*	*B*,[a] Å^2
Pt	0.67950 (8)	0.15829 (5)	0.32507 (3)	2.27 (1)
Os(1)	0.83550 (8)	0.24580 (5)	0.24794 (3)	2.95 (2)
Os(2)	0.55010 (8)	0.15857 (5)	0.21418 (3)	2.56 (2)
Os(3)	0.90416 (8)	0.07712 (5)	0.22356 (4)	3.05 (2)
S(1)	0.7477 (5)	0.1721 (3)	0.1650 (2)	3.1 (1)
S(2)	0.6906 (5)	0.0456 (3)	0.2633 (2)	2.5 (1)
P(1)	0.7045 (5)	0.0647 (3)	0.3976 (2)	2.9 (1)
P(2)	0.6136 (6)	0.2769 (3)	0.3684 (2)	3.1 (1)
C(1)	0.995 (2)	0.292 (1)	0.224 (1)	5.6 (6)*
C(1)	1.098 (2)	0.3181 (9)	0.2111 (7)	6.7 (4)*
C(2)	0.937 (2)	0.233 (1)	0.3183 (8)	4.0 (5)*
C(2)	1.018 (2)	0.2281 (9)	0.3609 (6)	5.6 (4)*
C(3)	0.754 (2)	0.354 (1)	0.2475 (9)	4.7 (5)*
O(3)	0.713 (2)	0.4255 (9)	0.2473 (6)	5.7 (4)*
C(4)	0.469 (2)	0.264 (1)	0.1844 (8)	4.1 (5)*
O(4)	0.420 (2)	0.3276 (9)	0.1675 (7)	6.1 (4)*
C(5)	0.453 (2)	0.095 (1)	0.1560 (8)	3.5 (4)*
C(5)	0.401 (2)	0.0551 (9)	0.1200 (7)	6.2 (4)*
C(6)	0.413 (2)	0.148 (1)	0.2606 (8)	3.9 (5)*
O(6)	0.317 (1)	0.1376 (8)	0.2835 (6)	5.1 (4)*
C(7)	1.055 (2)	0.112 (1)	0.1878 (9)	4.7 (5)*
O(7)	1.145 (2)	0.132 (1)	0.1621 (7)	6.6 (4)*
C(8)	1.027 (2)	0.043 (1)	0.2889 (9)	3.9 (5)*
O(8)	1.105 (2)	0.0277 (9)	0.3287 (6)	5.4 (4)*
C(9)	0.887 (2)	−0.030 (1)	0.1894 (9)	5.1 (5)*
O(9)	0.871 (2)	−0.096 (1)	0.1680 (7)	6.5 (4)*
C(10)	0.770 (2)	0.105 (1)	0.4673 (8)	3.3 (4)*
C(11)	0.711 (2)	0.082 (1)	0.513 (1)	5.3 (5)*
C(12)	0.776 (3)	0.120 (1)	0.565 (1)	5.9 (6)*
C(13)	0.891 (3)	0.170 (1)	0.570 (1)	5.9 (6)*
C(14)	0.949 (2)	0.196 (1)	0.524 (1)	5.2 (6)*
C(15)	0.894 (2)	0.166 (1)	0.4717 (9)	4.5 (5)*
C(16)	0.521 (2)	0.258 (1)	0.4275 (8)	3.3 (4)*
C(17)	0.579 (2)	0.285 (1)	0.4802 (9)	4.0 (5)*
C(18)	0.502 (2)	0.268 (1)	0.526 (1)	5.7 (6)*
C(19)	0.374 (2)	0.229 (1)	0.513 (1)	5.6 (6)*
C(20)	0.320 (3)	0.199 (1)	0.461 (1)	6.4 (6)*
C(21)	0.391 (2)	0.215 (1)	0.4166 (8)	3.9 (5)*
C(22)	0.829 (2)	−0.022 (1)	0.3934 (9)	4.5 (5)*
C(23)	0.541 (2)	0.010 (1)	0.4038 (8)	3.8 (5)*
C(24)	0.478 (2)	0.342 (1)	0.3245 (8)	3.9 (4)*
C(25)	0.753 (2)	0.353 (1)	0.3935 (9)	4.2 (5)*
C(31B)	0.918 (5)	−1.007 (3)	0.015 (2)	6 (1)*
C(33B)	0.707 (5)	−1.021 (3)	0.042 (2)	6 (1)*
C(32B)	0.884 (6)	0.049 (3)	0.045 (2)	8 (2)*
C(33A)	0.182 (8)	0.486 (5)	0.463 (3)	14 (2)*
C(32A)	0.130 (7)	0.058 (4)	0.010 (3)	11 (2)*
C(31A)	0.987 (9)	−1.047 (4)	−0.023 (3)	13 (3)*

[a] Values marked with an asterisk denote isotropically refined atoms.

Table VII. Interatomic Distances (Å) with Esd's for $PtOs_3(CO)_9(PMe_2Ph)_2(\mu_3\text{-}S)_2$ (**2**)

Pt–Os(1)	2.936 (1)	P(1)–C(23)	1.80 (2)
Pt–Os(2)	2.789 (1)	P(2)–C(16)	1.85 (2)
Pt–S(2)	2.334 (4)	P(2)–C(24)	1.84 (2)
Pt–P(1)	2.282 (5)	P(2)–C(25)	1.81 (2)
Pt–P(2)	2.274 (5)	C(1)–O(1)	1.15 (2)
Pt–C(2)	2.75 (2)	C(2)–O(2)	1.19 (2)
Pt–C(6)	2.76 (2)	C(3)–O(3)	1.18 (2)
Os(1)–Os(2)	3.027 (1)	C(4)–O(4)	1.14 (2)
Os(1)–Os(3)	2.798 (1)	C(5)–O(5)	1.13 (2)
Os(1)–S(1)	2.362 (5)	C(6)–O(6)	1.16 (2)
Os(1)–C(1)	1.87 (3)	C(7)–O(7)	1.19 (2)
Os(1)–C(2)	1.84 (2)	C(8)–O(8)	1.15 (2)
Os(1)–C(3)	1.85 (2)	C(9)–O(9)	1.16 (2)
Os(2)–S(1)	2.414 (5)	C(10)–C(11)	1.39 (3)
Os(2)–S(2)	2.406 (4)	C(11)–C(12)	1.45 (3)
Os(2)–C(4)	1.91 (2)	C(10)–C(15)	1.50 (3)
Os(2)–C(5)	1.85 (2)	C(12)–C(13)	1.33 (3)
Os(2)–C(6)	1.89 (2)	C(13)–C(14)	1.40 (3)
Os(3)–S(1)	2.396 (5)	C(14)–C(15)	1.40 (3)
Os(3)–S(2)	2.453 (5)	C(16)–C(17)	1.38 (3)
Os(3)–C(7)	1.89 (2)	C(16)–C(21)	1.40 (2)
Os(3)–C(8)	1.89 (2)	C(17)–C(18)	1.47 (3)
Os(3)–C(9)	1.86 (2)	C(18)–C(19)	1.34 (3)
P(1)–C(10)	1.83 (2)	C(19)–C(20)	1.39 (3)
P(1)–C(22)	1.81 (2)	C(20)–C(21)	1.39 (3)

Table VIII. Selected Interatomic Angles (deg) with Esd's for $PtOs_3(CO)_9(PMe_2Ph_2)(\mu_3\text{-}S)_2$ (**2**)

Os(1)–Pt–Os(2)	63.78 (3)	Os(3)–Os(1)–C(1)	93.3 (7)
Os(1)–Pt–S(2)	81.1 (1)	Os(3)–Os(1)–C(2)	89.7 (6)
Os(1)–Pt–P(1)	143.4 (1)	Os(3)–Os(1)–C(3)	164.9 (7)
Os(1)–Pt–P(2)	97.8 (1)	S(1)–Os(1)–C(1)	95.7 (7)
Os(2)–Pt–S(2)	55.2 (1)	S(1)–Os(1)–C(2)	143.9 (6)
Os(2)–Pt–P(1)	137.1 (1)	S(1)–Os(1)–C(3)	110.6 (7)
Os(2)–Pt–P(2)	110.1 (1)	Pt–Os(2)–C(4)	117.1 (6)
S(2)–Pt–P(1)	90.9 (2)	Pt–Os(2)–C(5)	146.4 (6)
S(2)–Pt–P(2)	164.2 (2)	Pt–Os(2)–C(6)	69.3 (6)
P(1)–Pt–P(2)	98.9 (2)	S(1)–Os(2)–C(4)	91.8 (6)
Pt–Os(1)–Os(2)	55.75 (2)	S(1)–Os(2)–C(5)	89.5 (6)
Pt–Os(1)–Os(3)	82.22 (3)	S(1)–Os(2)–C(6)	172.9 (6)
Pt–Os(1)–S(1)	100.7 (1)	S(2)–Os(2)–C(4)	167.3 (6)
Os(2)–Os(1)–Os(3)	75.64 (3)	S(2)–Os(2)–C(5)	99.2 (6)
Os(2)–Os(1)–S(1)	51.4 (1)	S(2)–Os(2)–C(6)	90.9 (6)
Os(3)–Os(1)–S(1)	54.6 (1)	Os(1)–Os(3)–C(7)	93.2 (6)
Pt–Os(2)–Os(1)	60.47 (3)	Os(1)–Os(3)–C(8)	102.3 (6)
Pt–Os(2)–S(1)	103.6 (1)	Os(1)–Os(3)–C(9)	158.8 (7)
Pt–Os(2)–S(2)	52.8 (1)	S(1)–Os(3)–C(7)	89.4 (7)
Os(1)–Os(2)–S(1)	49.9 (1)	S(1)–Os(3)–C(8)	155.7 (6)
Os(1)–Os(2)–S(2)	78.1 (1)	S(1)–Os(3)–C(9)	106.5 (7)
S(1)–Os(2)–S(2)	84.2 (2)	S(2)–Os(3)–C(7)	173.0 (6)
Os(1)–Os(3)–S(1)	53.4 (1)	S(2)–Os(3)–C(8)	92.4 (6)
Os(1)–Os(3)–S(2)	82.1 (1)	S(2)–Os(3)–C(9)	89.2 (7)
S(1)–Os(3)–S(2)	83.6 (2)	Os(1)–C(1)–O(1)	176 (2)
Os(1)–S(1)–Os(2)	78.7 (2)	Os(1)–C(2)–O(2)	171 (2)
Os(1)–S(1)–Os(3)	72.0 (1)	Os(1)–C(3)–O(3)	175 (2)
Os(1)–S(1)–Os(3)	96.1 (2)	Os(2)–C(4)–O(4)	179 (2)
Pt–S(2)–Os(2)	72.1 (1)	Os(2)–C(5)–O(5)	176 (2)
Pt–S(2)–Os(3)	103.9 (2)	Os(2)–C(6)–O(6)	172 (2)
Os(2)–S(2)–Os(3)	94.8 (2)	Os(3)–C(7)–O(7)	176 (2)
Pt–Os(1)–C(1)	156.0 (7)	Os(3)–C(8)–O(8)	176 (2)
Pt–Os(1)–C(2)	65.6 (6)	Os(3)–C(9)–O(9)	177 (2)
Pt–Os(1)–C(3)	99.7 (6)		

variable-temperature ^1H NMR study that revealed a rapid dynamical exchange process.[8] At 155 K the spectrum of **2** shows four broad singlets at $\delta = 2.36$, 1.79, 1.70, and 1.47 in the methyl region that can be attributed to the four inequivalent methyl groups; see Figure 4. As the temperature is raised, the resonances broaden and coalesce in pairs. The resonance at 2.36 ppm averages with the resonance at 1.79 ppm, and the resonance at 1.70 ppm averages with the resonance at 1.47 ppm. The coalescence temperature for the former pair appears to be 167 K. Due to the smaller shift separation of the latter pair, their coalescence temperature occurs few degrees lower. From the shift separation and coalescence temperature of the former pair, the rate of exchange and free energy of activation were estimated to be $R = 507\ s^{-1}$ and $\Delta G^* = 7.5$ kcal/mol, respectively. At higher temperatures the averaged resonances sharpen, and at 199 K coupling to the ^{31}P nuclei is observed in both resonances. At 25 °C coupling to the platinum isotope ^{195}Pt is observed: $J_{^{195}Pt-H} \sim 30$ Hz (see Table I).

It was found that **1** could be prepared also by the addition of a monoosmium unit to **2**. When solutions of **2** and $Os(CO)_5$ were irradiated with UV light, compound **1** was obtained in 18% yield. Unfortunately, the conversion of **2** was low, and 50% of compound **2** was recovered.

Discussion

In previous studies it has been shown that triosium carbonyl cluster complexes that contain triply bridging sulfido ligands readily add mononuclear metal-containing groups to yield higher nuclearity clusters.[4] In these studies it has been shown that the tetranuclear complexes **2** and **3** also capture mononuclear fragments to yield the pentanuclear compound **1**; see Scheme I. The structures of the M_4S_2 clusters of **2** and **3** are similar, except that **2** contains one metal–metal bond less than **3**.

It is believed that the lone pair of electrons on the sulfido ligands serve as the initial point of contact of the incoming metal unit

Scheme I

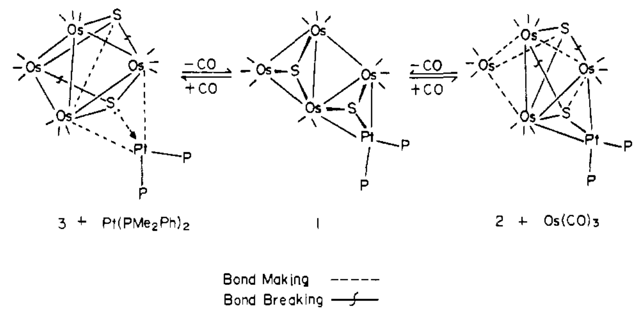

to the cluster through the formation of a donor–acceptor bond by using an empty metal orbital formed by the loss of a ligand. Several examples of such donor–acceptor bonds have been characterized recently.[20] PtL_4 (L = phosphine) complexes are known to dissociate ligands readily in solution.[21] The CO dissociation from $Os(CO)_5$ is promoted by UV irradiation. The formation of the donor–acceptor sulfur–metal bond may cause a weakening of metal–sulfur bonds in the cluster and facilitate their cleavage. The complete transformation probably involves several steps and details of all of these cannot be predicted at this time, but Scheme I shows the essential features of the bond-making and bond-breaking transformations. The tetranuclear clusters **2** and $Os_4(CO)_{13}(\mu_3\text{-}S)_2$ are formed competitively when **1** is treated with CO. It is believed that $Os_4(CO)_{13}(\mu_3\text{-}S)_2$ is formed from **3** generated initially in this reaction since **3** is known to add CO to form $Os_4(CO)_{13}(\mu_3\text{-}S)_2$ under these conditions.[18] Clearly, it is the loss of the platinum-containing subunit that leads to the tetraosmium product. It is most likely the loss of the osmium unit Os(4) (Figure 1) that leads to **2**. Overall, the two-step process **3** → **1** → **2** can be regarded as a metal–metal exchange reaction, eq 1, with compound **1** being a stable and isolable intermediate.

Compound **2** is a 64-electron cluster. It contains only four metal–metal bonds and is thus electron-precise. In contrast, compound **3**, which is also a 64-electron cluster, contains five metal–metal bonds. As a result, it is not possible to distribute the electrons in an arrangement of two-center two-electron bonds so that each metal atom has 18 electrons. However, the structure of **3** has been rationalized by the skeletal electron pair (SEP) theory.[22] Curiously, the compounds $WOs_3(CO)_{12}(PMe_2Ph)(\mu_3\text{-}S)_2$ and $WOs_3(CO)_{11}(PMe_2Ph)_2(\mu_3\text{-}S)_2$ exhibit this same dichotomy in bonding.[23] The former compound contains the closed structure while the latter one contains the open structure. Compound **2** could, in principle, adopt a structure that obeys the SEP theory simply by closing the Pt···Os(3) separation to a normal bonding distance, and with this in mind the NMR spectra of **2** will be discussed.

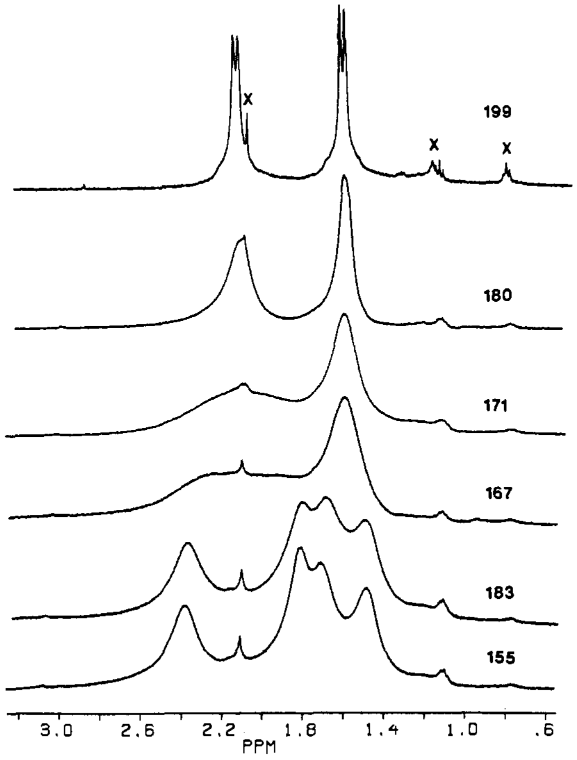

Figure 4. Variable-temperature ^1H NMR spectra of $PtOs_3(CO)_9(PMe_2Ph)_2(\mu\text{-}S)_2$ (**2**) in the methyl region. The small peaks labeled X are due to the unidentified trace impurities.

In the solid state the molecular structure of **2** contains no symmetry elements. Accordingly, the phosphine ligands are inequivalent. This is verified by the ^{31}P NMR spectrum, which shows two resonances that are coupled appropriately to each other

Scheme II

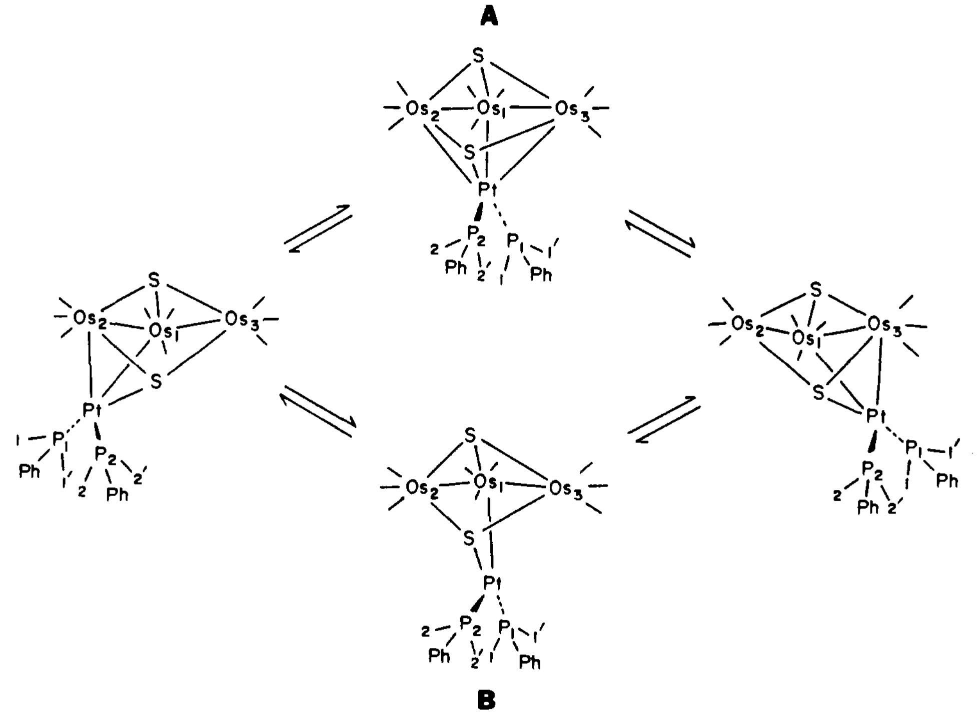

and to the naturally abundant ^{195}Pt nuclei. The ^1H NMR spectrum of **2** at 155 K shows four broad singlets in the aliphatic region that can be attributed to the four inequivalent methyl groups on the two PMe_2Ph ligands. A pairwise averaging is demonstrated by the broadening, coalescence, and sharpening into two singlets (doublets at 199 K due to ^{31}P-H coupling) shown by the spectra recorded at higher temperatures; see Figure 4. This indicates the presence of a dynamical process that produces a time-averaged plane of symmetry. Two processes that could explain all the observations are shown in Scheme II. Via mechanism A, a bond is formed between the platinum atom and the third osmium atom. The intermediate has the structure that is predicted to be stable by the SEP theory. Alternatively, via mechanism B a platinum–osmium bond is broken. The intermediate contains a 16-electron platinum atom. The two processes can not be distinguished with the available information. In fact, they are permutationally indistinguishable, but the distinction between bond-making and bond-breaking is certainly chemically and physically real. Intuitively, the bond-making process, A, is preferred because the averaging is very rapid, $\Delta G^{\ddagger}_{167} = 7.5$ kcal/mol, and this intermediate is expected to be a relatively stable one. Conversely, the bonding-breaking process, B, seems less likely since it seems that the metal–metal bond cleavage should have an activation barrier higher than 7.5 kcal/mol.[24]

Acknowledgment. This work was supported by the National Science Foundation, Grant No. CHE-8416460. NMR studies were supported by Grant No. CHE-8207445 from the National Science Foundation to the NMR Regional Facility at the University of South Carolina. We thank Drs. A. R. Garber and H. Cohen for their assistance in recording the variable-temperature NMR spectra.

Registry No. **1**, 101567-25-3; **2**, 101630-00-6; **3**, 82093-50-3; **4**, 72282-40-7; $Os_4(CO)_{13}(\mu_3\text{-}S)_2$, 83928-37-4; $Os_4(CO)_{11}(PMe_2Ph)(\mu_3\text{-}S)_2$, 91281-79-7; $Os_3(CO)_8(PMe_2Ph)(\mu_3\text{-}S)_2$, 101567-26-4; $Os_3(CO)_7(PMe_2Ph)_2(\mu_3\text{-}S)_2$, 101567-27-5; $Os(CO)_5$, 16406-49-8; $Pt(PMe_2Ph)_4$, 33361-89-6; Pt, 7440-06-4; Os, 7440-04-2.

Supplementary Material Available: Listings of anisotropic thermal parameters for both structures and additional interatomic angles for **2** (3 pages). Ordering information is given on any current masthead page. According to policy instituted Jan 1, 1986, the tables of calculated and observed structure factors (12 pages) are being retained in the editorial office for a period of 1 year following the appearance of this work in print. Inquiries for copies of these materials should be directed to the Editor.

---

(20) (a) Adams, R. D.; Horváth, I. T.; Wang, S. *Inorg. Chem.* **1985**, *24*, 1728. (b) Winter, A.; Jibril, I.; Huttner, G. *J. Organomet. Chem.* **1983**, *242*, 259.

(21) Taylor, R. C.; Young, J. F.; Wilkinson, G. *Inorg. Chem.* **1966**, *5*, 20.

(22) (a) Wade, K. In *Transition Metal Clusters*; Johnson, B. F. G., Ed.; Wiley: Chichester, England, 1980; Chapter 3. (b) Johnson, B. F. G.; Benfield, R. E. In *Topics in Stereochemistry*; Geoffroy, G. L., Ed.; Wiley: 1981, Vol. 12.

(23) Adams, R. D.; Horváth, I. T.; Mathur, P. *J. Am. Chem. Soc.* **1984**, *106*, 6296.

(24) See ref 1, Chapter 5.

Contribution from the Department of Chemistry,
University of South Carolina, Columbia, South Carolina 29208

Cluster Syntheses. 12. Metal–Metal Exchange Reactions. Systematics of the Synthesis of Platinum–Osmium Carbonyl Clusters Containing Quadruply Bridging Sulfido Ligands

Richard D. Adams,* James E. Babin, Rahina Mathab, and Suning Wang

Received November 14, 1985

The reaction of $Os_5(CO)_{15}(\mu_4\text{-}S)$ (**1**) heptahydrate, $Pt(PPh_3)_2C_2H_4$ has yielded several new platinum–osmium clusters containing quadruply bridging sulfido ligands and $Os_5(CO)_{14}(PPh_3)(\mu_4\text{-}S)$ (**3**). The three platinum–osmium clusters $PtOs_4(CO)_{13}(PPh_3)(\mu_4\text{-}S)$ (**2**), $PtOs_5(CO)_{15}(PPh_3)(\mu_4\text{-}S)$ (**4**), and $PtOs_5(CO)_{15}(PPh_3)_2(\mu_4\text{-}S)$ (**6**) have been characterized by single-crystal X-ray diffraction analyses. For **2**: space group $P\bar{1}$, $a = 13.116$ (4) Å, $b = 9.655$ (3) Å, $c = 14.669$ (4) Å, $\alpha = 89.68$ (3)°, $\beta = 104.79$ (2)°, $\gamma = 89.11$ (3)°, $Z = 2$, $\rho_{calcd} = 2.99$ g/cm^3. The structure was solved by the heavy-atom method and refined (4505 reflections) to the final residuals $R_F = 0.044$ and $R_{wF} = 0.052$. The molecule consists of a square-pyramidal cluster of four osmium atoms and one platinum atom with a quadruply bridging sulfido ligand on the square base. The platinum atom lies in the square base. For **4**: space group $P2_1/c$, $a = 8.986$ (7) Å, $b = 16.605$ (5) Å, $c = 26.005$ (8) Å, $\beta = 97.62$ (4)°, $Z = 4$, $\rho_{calcd} = 3.21$ g/cm^3. The structure of **4** was solved by direct methods and was refined (3947 reflections) to the final residuals $R_F = 0.040$ and ground = 0.048. The molecule consists of a square-pyramidal cluster of five osmium atoms with a quadruply bridging sulfido ligand on the square base and a $Pt(CO)PPh_3$ moiety bridging one of the triosmium triangles. For **6**: space group $P\bar{1}$, $a = 12.538$ (2) Å, $b = 15.908$ (2) Å, $c = 18.061$ (2) Å, $\alpha = 63.008$ (9)°, $\beta = 76.629$ (9)°, $\gamma = 65.68$ (1)°, $Z = 2$, $\rho_{calcd} = 2.45$ g/cm^3. The structure was solved by the heavy-atom method and was refined (4976 reflections) to the final residuals $R_F = 0.049$ and $R_{wF} = 0.065$. The molecule consists of a square-pyramidal cluster of four osmium atoms and one platinum atom with the base bridged by a quadruply bridging sulfido ligand and one of the osmium–osmium bonds in the square base bridged by an $Os(CO)_3(PPh_3)$ moiety. Compound **6** is believed to be an intermediate in the formation of **2**. **6** reacts with carbon monoxide to yield both **2** and **3**. The yield of **6** is increased when the reaction is performed in the presence of PPh_3. The yield of **4** is increased when the reaction is performed under CO. A scheme based on hexanuclear intermediates is proposed to explain the formation of all the products.

Introduction

Recent studies have shown that certain platinum alloys and bimetallic mixtures exhibit catalytic properties that are far superior to those of the homonuclear components.[1-3] These observations have stimulated an intense interest in the chemistry of heteronuclear transition-metal cluster compounds. Unfortunately, the synthetic routes to heteronuclear cluster compounds have been almost as wide ranging and varied in type as the compounds themselves are.[4]

In this report the synthesis of several new platinum–osmium clusters by the reaction of $Os_5(CO)_{15}(\mu_4\text{-}S)$ (**1**) with $Pt(PPh_3)_2C_2H_4$ will be described. Although lightly stabilized[5] and electron-deficient[6] osmium clusters will react with platinum

---

(1) (a) Sachtler, W. M. H. *J. Mol. Catal.* **1984**, *25*, 1. (b) Guczi, L. *J. Mol. Catal.* **1984**, *25*, 13. (c) Derovane, E. G. *J. Mol. Catal.* **1984**, *25*, 51.

(2) (a) Fukushima, T.; Arakawa, H.; Ichikawa, M. *J. Chem. Soc., Chem. Commun.* **1985**, 729. (b) Ellgen, P. C.; Bartley, W. J.; Bhasin, M. M.; Wilson, T. P. *Adv. Chem. Ser.* **1979**, *No. 178*, 147.

(3) Knifton, J. F. *J. Chem. Soc., Chem. Commun.* **1983**, 729.

(4) (a) Roberts, D. A.; Geoffroy, G. L. In *Comprehensive Organometallic Chemistry*; Wilkinson, G., Stone, F. G. A., Eds.; Pergamon: Elmsford, NY, 1982; Chapter 40. (b) Bruce, M. I. *J. Organomet. Chem.* **1983**, *257*, 417.

(5) Couture, C.; Farrar, D. H. *J. Chem. Soc., Chem. Commun.* **1985**, 197.

(6) Farrugia, L. J.; Howard, J. A. K.; Mitrprachachon, P.; Stone, F. G. A.; Woodward, P. *J. Chem. Soc., Dalton Trans.* **1981**, 155.

0020-1669/86/1325-1623$01.50/0